Geophysical and Astrophysical Fluid Dynamics
Vol. 00, No. 00, Month 2009, 1–11

An analytic interface dynamo over a shear layer of finite depth

K. Petrovay†*, A. Kerekes‡ and R. Erdélyi‡

†Eötvös University, Department of Astronomy, Budapest, Pf. 32, H-1518 Hungary, and
ASIAA/National Tsing Hua University - TIARA, Hsinchu, Taiwan
‡SP^{2}RC, Dept. of Applied Mathematics, Univ. of Sheffield, Hicks Building, Hounsfield Road, Sheffield S3 7RH, UK

()

Parker's analytic Cartesian interface dynamo is generalized to the case of a shear layer of finite thickness and low resistivity ("tachocline"), bounded by a perfect conductor ("radiative zone") on the one side, and by a highly diffusive medium ("convective zone") supporting an α-effect on the other side. In the limit of high diffusivity contrast between the shear layer and the diffusive medium, thought to be relevant for the Sun, a pair of exact dispersion relations for the growth rate and frequency of dynamo modes is analytically derived. Graphic solution of the dispersion relations displays a somewhat unexpected, non-monotonic behaviour, the mathematical origin of which is elucidated. The dependence of the results on the parameter values (dynamo number and shear layer thickness) is investigated. The implications of this result for the solar dynamo problem are discussed.

Keywords: MHD; dynamo; Sun: interior; Sun: magnetic fields

1 Introduction

Interface dynamos are a widely discussed class of astrophysical dynamos, especially in the solar context (Petrovay 2000, Solanki *et al.* 2006, Charbonneau 2005). In contrast to the textbook case of Parker's migratory dynamo, in an interface dynamo the α and Ω effects operate in spatially distinct but adjacent layers. In this setup the dynamo wave will arise as a surface wave propagating along the interface of the two regions. While dynamo problems with spatially separated α and Ω had been considered since the 1970's (see e.g. the references in Zeldovich *et al.* 1984), the classic analytic formulation of the problem is due to Parker (1993).

It has long been suspected (Parker 1975, Schüssler 1984, Petrovay 1991), and recently demonstrated in numerical simulations (Browning *et al.* 2006) that the toroidal magnetic flux generated in the solar dynamo can only be stored below the base of the convective zone proper, as various flux transport effects (buoyancy and pumping) remove it quite effectively from the convective zone. With the discovery of the tachocline layer it became clear that this hypothetical flux reservoir coincides with the strongest rotational shear in the solar interior, which is plausibly also responsible for the production of the strong toroidal magnetic fields, i.e. that this is the site of the Ω-effect. The site and nature of the α-effect is much less clear; in interface dynamo models it is assumed to be concentrated in the deep convective zone, just above the tachocline.

Current helioseismic evidence indicates that at low heliographic latitudes the tachocline is situated immediately below the adiabatically stratified convective zone. (At higher latitudes some overlap may be present.) This suggests that the tachocline is much less turbulent than the convective zone proper. This is also consistent with another physical consideration: the high overall toroidal field strength that must be present if all the magnetic flux emerging during a solar cycle resides in the thin tachocline layer should strongly suppress turbulence there. The strong subadiabatic stratification of the tachocline will then inhibit the penetration of meridional circulation to it, presenting a difficulty for flux transport models, the main contender of interface dynamo models.

*Corresponding author. E-mail: K.Petrovay@astro.elte.hu

Geophysical and Astrophysical Fluid Dynamics
ISSN: 0309-1929 print/ISSN 1029-0419 online © 2009 Taylor & Francis
DOI: 10.1080/03091920xxxxxxxxx

There is some disagreement over whether the oscillatory magnetic field generated by the dynamo pervades the whole of the tachocline or not. For effective magnetic diffusivities less than $10^8\,\mathrm{cm}^2/\mathrm{s}$ or so, the penetration depth (skin depth) of the oscillatory magnetic field is much less than the helioseismically inferred tachocline thickness (order of 10 Mm), so the penetration cannot be complete. In this "slow tachocline" scenario (Garaud 2001, Brun and Zahn 2006) the dynamical changes in the bulk of the tachocline take place on the long diffusive timescale. In the alternative "fast tachocline" scenario (Forgács-Dajka and Petrovay 2001, 2002, Forgács-Dajka 2003), hydrodynamical instabilities maintain some modest level of turbulence in the tachocline, so the resulting higher skin depth allows the dynamo field to penetrate deeper. In this case it is the Lorentz force in the dynamo generated field that limits the penetration of differential rotation deeper into the radiative interior, so tachocline thickness and skin depth are intimately related and should agree within an order of unity factor (Petrovay 2003). In the present paper we will consider the fast tachocline case; some observational support for this scenario comes from the recent detection of solar cycle related changes in tachocline properties (Baldner and Basu 2008), as predicted by the fast tachocline models.

The interface dynamo option for the solar dynamo is attractive, as it would explain the high ($\sim 100\,\mathrm{kG}$) field strength of toroidal fields and their equatorward propagation, while still being consistent with physical assumptions about the magnetic diffusivity values in both the convective zone and tachocline and about the meridional flow amplitude. Interface dynamo models for the Sun have been constructed, e.g., by Charbonneau and MacGregor (1997), Tobias (1996) or Markiel and Thomas (1999). Unfortunately, none of these models show a compelling detailed agreement with observed features of the cycle. Their main alternative, the flux transport dynamos (Dikpati and Charbonneau 1999, Chatterjee *et al.* 2004), in contrast, are more straightforward to parameterize so that they can reproduce some salient features of the solar cycle reasonably well; however, the physical consistency of the models is very much in doubt, especially regarding their assumptions on diffusive and advective magnetic flux transport processes (Choudhuri 2008).

The now classic analytic Parker (1993) interface dynamo consisted of two adjacent semiinfinite domains: one highly diffusive domain home to the α-effect and another, low diffusivity domain characterized by strong shear. As we have seen, the solar tachocline, corresponding to the shear layer in the Cartesian interface dynamo, has a quite limited thickness, so it is not particularly well represented by a semiinfinite domain. The aim of the present paper is to generalize Parker's analytical interface dynamo to the case when the shear layer has a finite thickness.

What makes this problem particularly relevant is the recent proposal (Petrovay 2007) that combining an interface model with a fast tachocline scenario both the magnetic field amplitude and the thickness of the tachocline can be determined (in the simplest case, by solving two algebraic equations). Under some plausible assumptions, two solutions are found: one with strong field and thin tachocline and another one with weaker field and a thicker tachocline. These represent "high" and "low" states of solar activity, suggesting a link with the phenomenon of grand minima. Based on an analogy with surface gravity waves, this model assumed that a finite shear layer thickness h reduces the growth rate of the interface dynamo by a factor $\tanh(hk)$, where k is the wave number. One objective of the present work is to examine the validity of this assumption.

We note that interface dynamos with finite shear layers have previously been considered in many numerical implementations (e.g. Charbonneau and MacGregor 1997, Markiel and Thomas 1999) as well as in a semianalytic Cartesian setup more general than our current model (Zhang *et al.* 2004). The effect of varying h, however, was not studied in any of those models, due to the large number of other free parameters and to the different focus of those papers. It is therefore legitimate to consider a setup where h is a variable parameter while in other respects the model is kept as simple as possible.

The structure of our paper is as follows. In section 2 we analytically derive the dispersion relations in the limit relevant to the Sun. Section 3 presents graphical solutions of these dispersion relations and discusses their properties. Finally section 4 concludes the paper.

2 Derivation of the Dispersion Relations

2.1 *Generic complex dispersion relations*

We use a Cartesian setup where the coordinate z corresponds to height above the bottom of the convective zone in the solar application, while x and y correspond to heliographic latitude and longitude, respectively. Let η denote the magnetic diffusivity, α the α parameter of dynamo theory (see e.g. Petrovay 2000) and $\Omega = dv_y/dz$ the shear rate of the velocity field representing radial differential rotation. The magnetic field is decomposed into a "toroidal" component B_y and a "poloidal" component $\nabla \times A_y \mathbf{e}_y$ where A_y is the toroidal vector potential.

Consider now the following 3-layer "sandwich" setup:

Convective zone	$z > 0$	$\eta = \eta_+$	$\alpha \neq 0$	$\Omega = 0$	$B_y = B(x,z,t)$	$A_y = A(x,z,t)$
Tachocline	$-h < z < 0$	$\eta = \eta_-$	$\alpha = 0$	$\Omega \neq 0$	$B_y = b(x,z,t)$	$A_y = a(x,z,t)$
Radiative interior	$z < -h$	$\eta = 0$	$\alpha = 0$	$\Omega = 0$	$B_y = 0$	$A_y = 0$

The parameters η_+, η_-, α and Ω are assumed to be constant in their respective layers.

The $\alpha\Omega$ dynamo equations in $z > 0$ then read

$$\frac{\partial B}{\partial t} - \eta_+ \left(\frac{\partial^2 B}{\partial x^2} + \frac{\partial^2 B}{\partial z^2} \right) = 0, \tag{1a}$$

$$\frac{\partial A}{\partial t} - \eta_+ \left(\frac{\partial^2 A}{\partial x^2} + \frac{\partial^2 A}{\partial z^2} \right) = \alpha B, \tag{1b}$$

while in the tachocline we have

$$\frac{\partial b}{\partial t} - \eta_- \left(\frac{\partial^2 b}{\partial x^2} + \frac{\partial^2 b}{\partial z^2} \right) = \Omega \frac{\partial a}{\partial x}, \tag{2a}$$

$$\frac{\partial a}{\partial t} - \eta_- \left(\frac{\partial^2 a}{\partial x^2} + \frac{\partial^2 a}{\partial z^2} \right) = 0. \tag{2b}$$

The matching conditions at $z = 0$ are

$$b = B, \qquad a = A, \qquad \frac{\partial a}{\partial z} = \frac{\partial A}{\partial z}, \qquad \eta_- \frac{\partial b}{\partial z} = \eta_+ \frac{\partial B}{\partial z}, \tag{3a,b,c,d}$$

while at $z = -h$ they simply read

$$b = 0, \qquad a = 0. \tag{4a,b}$$

Following the standard procedure for the analytical solution of interface dynamo equations (Parker 1993, Petrovay and Kerekes 2004), for the solutions in terms of our variables $f(x,z,t)$ we consider normal modes of the form $f(z)\exp[(\sigma + \mathrm{i}\omega)t + \mathrm{i}kx]$. In $z > 0$, the z-dependent part $f(z)$ is sought in the form

$$B = C\mathrm{e}^{-Rz} \qquad A = (D + Ez)\mathrm{e}^{-Rz}, \tag{5a,b}$$

where $R = S + \mathrm{i}Q$, and C, σ, ω, k, S and Q are all real, while D and E are complex. As we expect the field to vanish as $z \to \infty$, S must be positive.

In the shear layer the solutions have a similar form, but, owing to the finite thickness of the layer, the solution is in general a superposition of modes growing and decaying with z:

$$a = (J\mathrm{e}^{rz} + J_1\mathrm{e}^{-rz}), \qquad b = (L + Mz)\mathrm{e}^{rz} + (L_1 + M_1 z)\mathrm{e}^{-rz}, \tag{6a,b}$$

where $r = s + \mathrm{i}q$ with s and q real and $s > 0$, as before. Equations (4a,b) then imply

$$J_1 = -J\mathrm{e}^{-2rh}, \qquad L_1 = hM_1 + (hM - L)\mathrm{e}^{-2hr}, \tag{7a,b}$$

respectively.

Substitution of our trial solutions (5a,b), (6a,b) into the four interface fitting conditions (3a-d) yields

$$J(1 - \mathrm{e}^{-2hr}) = D, \tag{8a}$$
$$L(1 - \mathrm{e}^{-2hr}) + h(M\mathrm{e}^{-2hr} + M_1) = C, \tag{8b}$$
$$rJ(1 + \mathrm{e}^{-2hr}) = E - DR, \tag{8c}$$
$$\eta_- \left[rL(1 + \mathrm{e}^{-2hr}) + M + M_1 - rh(M\mathrm{e}^{-2hr} + M_1)\right] = -\eta_+ RC. \tag{8d}$$

On the other hand, substituting (7a,b) into the trial solutions (5a,b) and (6a,b), and substituting these into the dynamo equations (1a,b), (2a,b) we obtain the dispersion relations

$$\eta_+ R^2 = \sigma + \mathrm{i}\omega + \eta_+ k^2, \tag{9a}$$
$$\eta_- r^2 = \sigma + \mathrm{i}\omega + \eta_- k^2, \tag{9b}$$
$$E = \alpha C/2\eta_+ R, \tag{9c}$$
$$-2\eta_- r(M\mathrm{e}^{rz} - M_1\mathrm{e}^{-rz}) = \mathrm{i}k\Omega J(\mathrm{e}^{rz} - \mathrm{e}^{-rz}\mathrm{e}^{-2hr}) \tag{9d}$$

the last of which implies the two separate relations

$$M = -\mathrm{i}k\Omega J/2\eta_- r, \qquad M_1 = M\mathrm{e}^{-2hr}. \tag{10a,b}$$

Using the relations (8a-c), as well as (9c,d), equation (8d) can be written as

$$rR(\mu^2 r + R\delta)(r + R\delta)/k^4 = \tfrac{1}{4}\mathrm{i}N[\delta - (1 - \delta^2)hr], \tag{11}$$

where we introduced the dynamo number $N = \alpha\Omega/\eta_+^2 k^3$ and the notation $\delta = \tanh(hr)$. Equation (11) establishes a relation between the complex vertical wavenumbers r and R. A second such relation is derived by eliminating $(\sigma + \mathrm{i}\omega)$ from equations (9a,b):

$$R^2 = \mu^2 r^2 - (\mu^2 - 1)k^2, \tag{12}$$

where the diffusivity contrast $\mu^2 = \eta_-/\eta_+$ was introduced.

Given the parameters N, μ and δ (or, equivalently, h) defining the problem, the pair of complex dispersion relations (11), (12) can in principle be solved for r and R. The frequency ω and growth rate σ of the dynamo wave then follow from (9a,b). The nine parameters C, D, E, J, J_1, L, L_1, M and M_1 are then determined by the relations (7)–(8c) and (9c,d). Substituting these into (5a,b), (6a,b) together with the derived values of r and R finally should yield the full z-dependence of the solution for a given value of k.

2.2 *Solar limit*

Unfortunately, an attempt to actually implement this procedure analytically encounters difficulties. Equations (11), (12) look deceivingly simple, yet the actual calculation soon becomes quite involved. To make progress, from this point onwards we restrict attention to the limit relevant for the solar interior.

In the solar convective zone the dynamo wave number and frequency are empirically known to be of order $k \sim 1/R_\odot$ and $\omega \sim \eta_+/R_\odot^2 \sim \eta_+ k^2$, where $R_\odot$ is the solar radius. In the tachocline below, the magnetic diffusivity is uncertain but surely several orders magnitude lower than the fixed value η_+: we may then safely take the limit $\eta_- \to 0$. With the fixed values of η_+, k and ω given above, the penetration depth (skin depth) of the oscillatory dynamo magnetic field will be $(2\eta_-/\omega)^{1/2} \sim \mu/k$, which also implies $|r| \sim k/\mu$. As the thickness h of a fast tachocline is expected to be a few skin depths, so in this limit we also expect $h \sim \mu/k \to 0$, suggesting the use of a fixed nondimensional layer depth $H = hk/\mu$ instead. Finally, inspection of equation (11) shows that the leading terms on the left-hand side will be of order $1/\mu^2$, while those on the right-hand side are of order N. So in order to keep the dynamo supercritical in the solar limit we need to keep $\mu^2 N$ fixed.

Summing up these considerations, the limit relevant to the solar case is

$$\mu \to 0, \qquad \text{while} \qquad H = hk/\mu = \text{finite} \qquad \text{and} \qquad \mathcal{N} = \mu^2 N = \text{finite}. \tag{13}$$

Equation (12) then simplifies to

$$R = (\mu^2 r^2 + k^2)^{1/2}\,. \tag{14}$$

Substituting this into (11) yields an equation for the complex wavenumber r only. In analogy with the nondimensional layer depth H, we now introduce the nondimensional equivalent of r as $\Psi = \mu r/k$: clearly, Ψ will remain finite in the solar limit, as discussed above. Expressing r with Ψ and keeping only leading order terms in the limit of $\mu \to 0$, equation (11) finally takes the form

$$\left[\Psi^2(\delta^2-1)^2H^2 + 2\Psi\delta(\delta^2-1)H + \delta^2\right]\mathcal{N}^2/16 + \mathrm{i}\Psi^2(\Psi^2-1)\delta\left[\Psi(\delta^2-1)H + \delta\right]\mathcal{N}/2 = \delta^2\Psi^4(1+\Psi^2)^2. \tag{15}$$

In this equation, Ψ and δ are complex, while the parameters $\mathcal{N}$ and H are real. We write δ and Ψ explicitly as

$$\delta = \delta_R + i\delta_I, \qquad \Psi^2 = \tilde{\sigma} + i\nu, \tag{16a,b}$$

where

$$\tilde{\sigma} = \sigma/\eta_+k^2, \qquad \nu = \omega/\eta_+k^2 \tag{17a,b}$$

are the dimensionless growth rate and frequency of the dynamo wave, and (16b) follows from (9b) in the limit $\mu \to 0$.

Upon performing these substitutions, equation (15) is split into real and imaginary parts. (The calculation is very tedious but still manageable by numerical algebra packages.) This finally yields two dispersion relations for the nondimensional growth rate $\tilde{\sigma} = \beta - 1$ and the nondimensional frequency ν. These are of the form

$$f_1(\tilde{\sigma}, \nu; H, \mathcal{N}) = 0, \qquad f_2(\tilde{\sigma}, \nu; H, \mathcal{N}) = 0, \tag{18a,b}$$

where

$$f_1(\tilde{\sigma}, \nu; H, \mathcal{N}) \equiv (a_{11}H^2 - a_{12})\mathcal{N}^2 + b_1\mathcal{N} + c_1, \qquad f_2(\tilde{\sigma}, \nu; H, \mathcal{N}) \equiv (a_{21}H^2 - a_{22})\mathcal{N}^2 + b_2\mathcal{N} + c_2 \tag{19a,b}$$

with

$$a_{11} = \nu(1+\delta_R^4+\delta_I^4) - 4\tilde{\sigma}\delta_R\delta_I(1-\delta_R^2+\delta_I^2) - 2\nu(\delta_R^2+3\delta_R^2\delta_I^2-\delta_I^2), \tag{20a}$$

$$a_{12} = 2\delta_I\delta_R, \tag{20b}$$

$$b_1 = 8[2\nu(1+2\tilde{\sigma})\delta_R\delta_I - (\tilde{\sigma}^2+\tilde{\sigma}-\nu^2)(\delta_R^2-\delta_I^2)], \tag{20c}$$

$$c_1 = 32[(\tilde{\sigma}^2+\tilde{\sigma}-\nu^2)\delta_R - \nu(2\tilde{\sigma}+1)\delta_I][(\tilde{\sigma}^2+\tilde{\sigma}-\nu^2)\delta_I + \nu(2\tilde{\sigma}+1)\delta_R], \tag{20d}$$

$$a_{21} = \tilde{\sigma}(1+\delta_R^4+\delta_I^4) - 4\nu\delta_R\delta_I(1-\delta_R^2+\delta_I^2) - 2\tilde{\sigma}(\delta_R^2+3\delta_R^2\delta_I^2-\delta_I^2), \tag{20e}$$

$$a_{22} = \delta_R^2 - \delta_I^2, \tag{20f}$$

$$b_2 = 8[\nu(1+2\tilde{\sigma})(\delta_R^2-\delta_I^2) + 2(\tilde{\sigma}^2+\tilde{\sigma}-\nu^2)\delta_R\delta_I], \tag{20g}$$

$$\begin{aligned} c_2 = 16[&\tilde{\sigma}(\tilde{\sigma}+1)(\delta_R-\delta_I) - \nu(\nu+1)\delta_R + \nu(\nu-1)\delta_I] \\ &\times[\tilde{\sigma}(\tilde{\sigma}+1)(\delta_R+\delta_I) - \nu(\nu-1)\delta_R + \nu(\nu+1)\delta_I]. \end{aligned} \tag{20h}$$

Recalling that $\delta = \tanh(hr) = \tanh(H\Psi)$, the real and imaginary parts of δ are

$$\delta_R = \frac{\cosh(H\tilde{s})\sinh(H\tilde{s})}{\cosh^2(H\tilde{s}) - \sin^2(H\tilde{q})}, \qquad \delta_I = \frac{\cos(H\tilde{q})\sin(H\tilde{q})}{\cosh^2(H\tilde{s}) - \sin^2(H\tilde{q})}, \tag{21a,b}$$

where $\tilde{s} = \mu s/k$ and $\tilde{q} = \mu q/k$ are related to $\tilde{\sigma}$ and ν by virtue of equations (9a,b):

$$\tilde{s}^2 = \tfrac{1}{2}[\tilde{\sigma} + (\tilde{\sigma}^2+\nu^2)^{1/2}], \qquad \tilde{q}^2 = \frac{\nu^2}{\tilde{\sigma} + [\tilde{\sigma}^2+\nu^2]^{1/2}}. \tag{22a,b}$$

It is straightforward to check that, in the limit $H \to \infty$ (i.e. $\delta \to 1$), Parker's original solution is retrieved (cf. equations (60), (61) in Parker 1993).

3 Solution

While the equations (18a,b) are quadratic in $\mathcal{N}$, they are in general extremely complicated functions of the other variables. Nevertheless, equations (18a,b) lend themselves most readily to a graphic solution. Fixing the value of the control parameters $\mathcal{N}$ and H, solutions correspond to the crossing points of the zero contours of functions f_1 and f_2 in the $\nu\tilde{\sigma}$ plane. Then, varying H while keeping either $\mathcal{N}$ or the total shear fixed one can study how the solutions deviate from the Parker solution ($H \to \infty$ limit) for finite values of H.

For the purposes of this study we take the "textbook" case $\mathcal{N} = 12\sqrt{2}$, already considered by Parker (1993). In the limit $H \to \infty$, considered by Parker, there is only one growing mode characterized by $\tilde{\sigma} = 1$ and $\nu = \sqrt{2}$, as borne out in figure 1*a*. As H is decreased, the solution bifurcates, and two sequences of apparently growing modes appear. Recall, however, that during the derivation of the dispersion relations in section 2, several steps may have resulted in the appearance of spurious solutions. Indeed, on physical grounds we expect to return Parker's solution in the $H \to \infty$ limit but also to behave as $\tilde{\sigma} \to 0$ at some finite positive value of H. On the basis of this consideration we must reject the "upper" (i.e. higher growth rate) sequence of solutions in figure 1, converging to $\tilde{\sigma} = 1.67$, $\nu = 2.01$, as spurious. The lower sequence, representing physical growing modes, in turn disappears for $H < 1.45$, i.e. the dynamo is suppressed for such low layer depths.

The variation of $\tilde{\sigma}$ with H is shown in figure 2. The variation can be roughly represented by a shifted tangent hyperbolic function. This was to be expected in analogy with surface gravity waves (Petrovay 2007), the shift here being due to the suppression of growing modes at a final layer depth. The detailed behaviour of the solution is, however, considerably richer that this simple theoretical expectation, displaying a surprising non-monotonic modulation. This is a real physical interference effect, due to the interaction of the waves

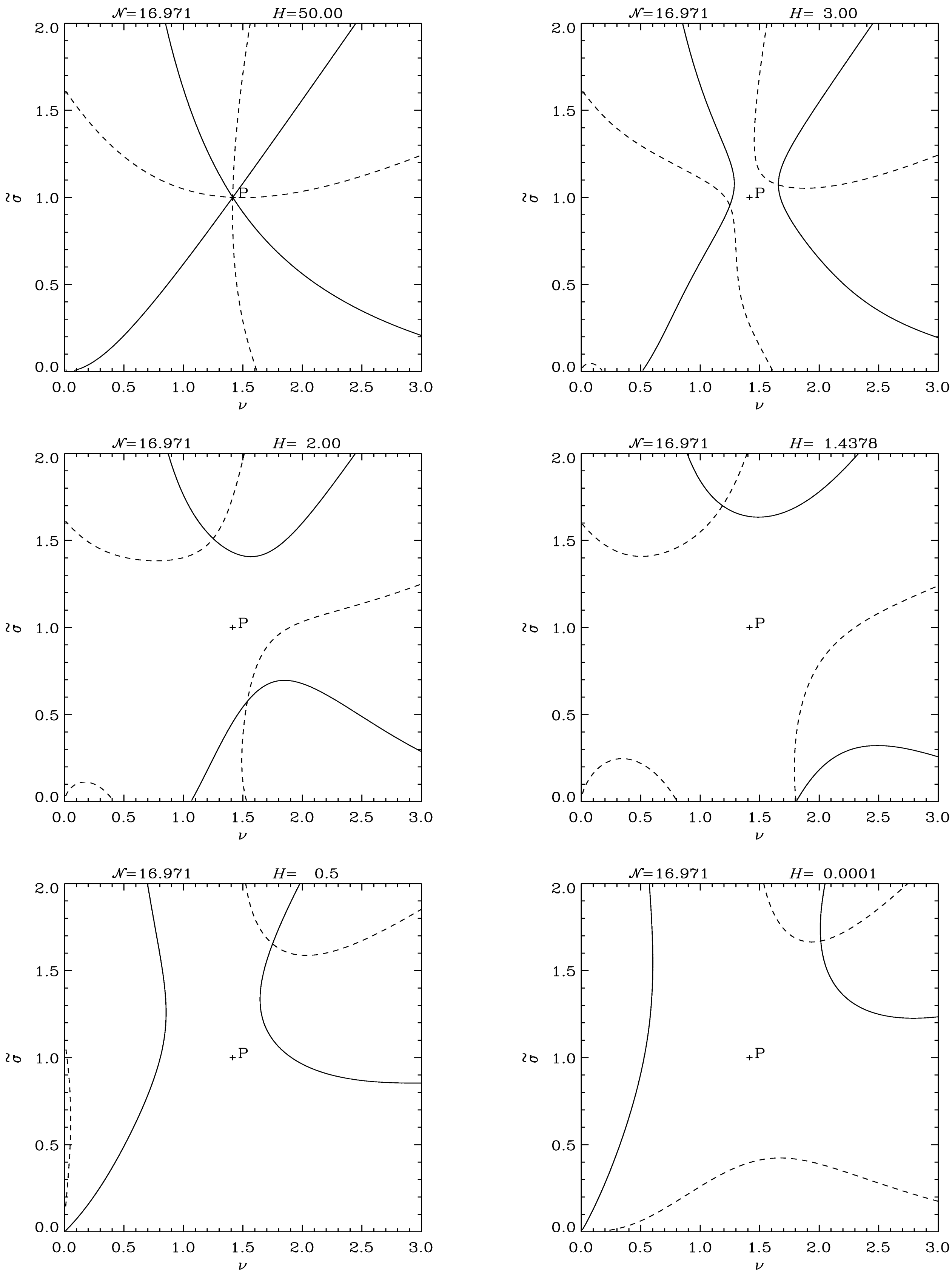

Figure 1. Zero contours of the functions f_1 (solid) and f_2 (dashed) on the $\nu\tilde{\sigma}$ plane, for different values of the layer depth H. Crossing points of the solid and dashed curves represent formal solutions of the dispersion relations. The solution in the limit $H \to \infty$ is marked by P.

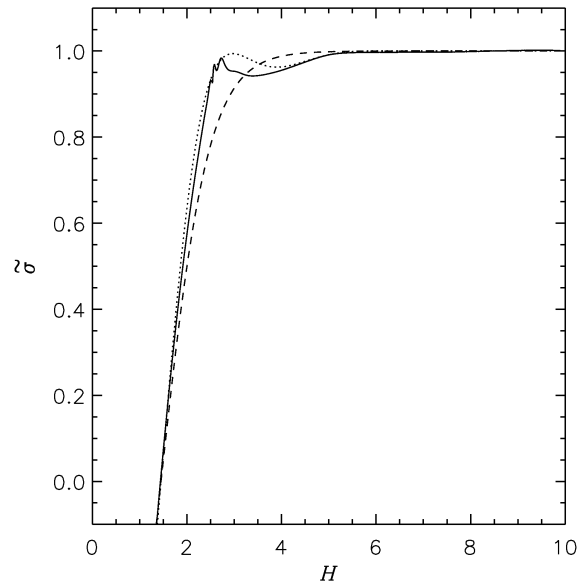

Figure 2. Variation of the nondimensional growth rate $\tilde{\sigma}$ with layer depth H for $\mathcal{N} = 12\sqrt{2}$. The solution is analytically fitted by a simple shifted tangent hyperbolic (dashed), on which a Gaussian damped sinusoidal is superposed (dotted).

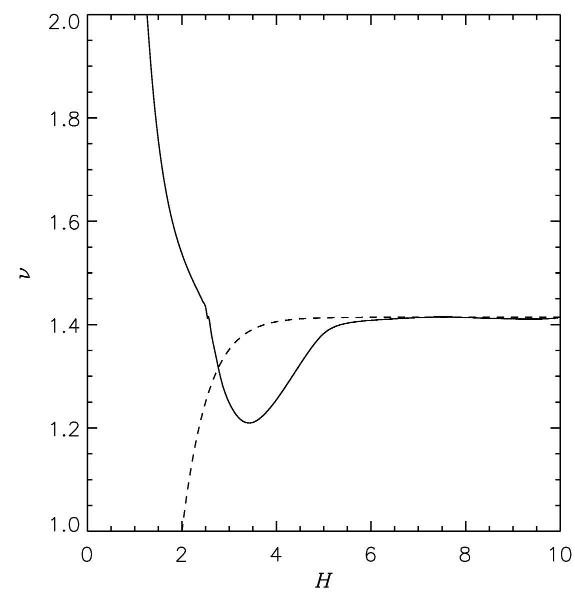

Figure 3. Variation of the nondimensional frequency ν with layer depth H for $\mathcal{N} = 12\sqrt{2}$. The relation $\nu^2 \propto \tanh(H)$ (dashed), based on an analogy with surface gravity waves, is shown for comparison.

originating at the interface and the waves reflected from the bottom of the tachocline. To imitate this modulation, we superpose an exponentially damped sinusoidal on the tangent hyperbolic to arrive at the following fitting function

$$\tilde{\sigma} = \tanh(H') + 0.2\sin(1.5H')\exp(-0.25H'^2), \qquad \text{where} \qquad H' = H - 1.45. \tag{23a,b}$$

Note, however, that the appearence and details of such interference effects may be sensitive to the details of the model setup (i.e. to how sharp the bottom of the tachocline is supposed to be).

The breakdown of the water wave analogy is even more apparent from figure 3. The variation of the frequency with layer depth is clearly quite different for interface dynamo waves than the simple $\nu^2 \propto$

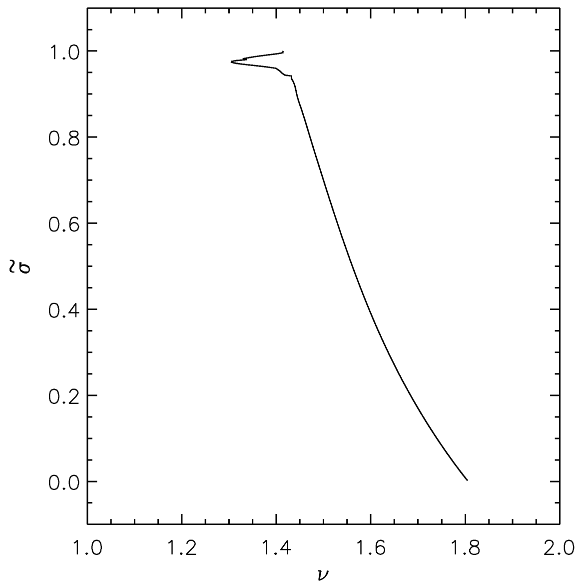

Figure 4. Trajectory of the physical solution sequence in the $\nu\tilde{\sigma}$ plane for varying H when $\mathcal{N} = 12\sqrt{2}$ is kept fixed

tanh(H) relation (dashed), valid for surface gravity waves.

Figure 4 presents the trajectory of the solution in the $\nu\beta$ plane. It is apparent that in the critical case $\nu \simeq 1.8$, at least an order of magnitude higher than the value $(2/N)^{1/2}$ suggested by Parker's original analysis.

4 Conclusion

In this paper we have generalized the textbook interface dynamo model of Parker (1993) to the case of finite tachocline thickness, while otherwise keeping the model as simple as possible. We found that the growth rate of the dynamo has a shifted tangent hyperbolic dependence on the layer depth, in agreement with the expectation based on an analogy with surface gravity waves. This finding lends some support to the claim (Petrovay 2007) that the combination of a fast tachocline and an interface dynamo can give rise to bimodal solutions, possibly explaining the phenomenon of grand minima. Under the assumption that the growth rate of the dynamo has a dependence on the tachocline depth similar to what was found in the present paper, in that previous work two solutions were found for a nonlinear interface dynamo combined with a fast tachocline: a strong field, thin tachocline solution corresponding to normal solar activity and a weak field, thick tachocline solution that may potentially represent a grand minimum state of solar acivity.

Yet the behaviour of the solutions does show some surprising features. The nondimensional frequency varies with layer depth in a non-intuitive way and the detailed behaviour of the growth rate—layer depth curve displayes a non-monotonic, oscillatory behaviour. This illustrates the richness of phenomena appearing even in strongly simplified interface dynamo models. A further systematic study of models of this type and of more generic models is needed to more fully explore the parameter space and to obtain a deeper understanding of the spectrum of possible dynamo solutions in an interface setup. Without such systematic studies no final verdict on the viability of an interface-type solution to the solar dynamo problem is possible.

Acknowledgments

This research was supported by the Hungarian Science Research Fund (OTKA) under grant no. K67746; by the European Commission through the SOLAIRE Network (MTRN-CT-2006-035484); by the Theoretical Institute for Advanced Research in Astrophysics (TIARA) operated under Academia Sinica and the National Science Council Excellence Projects program in Taiwan administered through grant number NSC95-2752-M-007-006-PAE; as well as by the Science and Technology Facilities Council (STFC), UK and the Mathematics and Statistics Research Centre (MSRC) of the University of Sheffield. K.P. acknowledges the warm hospitality received at the Department of Applied Mathematics, University of Sheffield during his visit. R.E. acknowledges M. Kéray for patient encouragement.

REFERENCES

Baldner, C.S. and Basu, S., Solar cycle related changes at the base of the convection zone. *Astrophys. J.* 2008, **686**, 1349–1361.

Browning, M.K., Miesch, M.S., Brun, A.S. and Toomre, J., Dynamo action in the solar convection zone and tachocline: Pumping and organization of toroidal fields. *Astrophys. J. Lett.* 2006, **648**, L157–L160.

Brun, A.S. and Zahn, J.P., Magnetic confinement of the solar tachocline. *Astron. Astrophys.* 2006, **457**, 665–674.

Charbonneau, P., . *Living Rev. Sol. Phys.* 2005, **2**, 2.

Charbonneau, P. and MacGregor, K.B., Solar interface dynamos II. Linear, kinematic models in spherical geometry. *Astrophys. J.* 1997, **486**, 502–520.

Chatterjee, P., Nandy, D. and Choudhuri, A.R., Full-sphere simulations of a circulation-dominated solar dynamo: Exploring the parity issue. *Astron. Astrophys.* 2004, **427**, 1019–1030.

Choudhuri, A.R., How far are we from a "Standard Model" of the solar dynamo? *Adv. Space Res.* 2008, **41**, 868–873.

Dikpati, M. and Charbonneau, P., A Babcock-Leighton flux transport dynamo with solar-like differential rotation. *Astrophys. J.* 1999, **518**, 508–520.

Forgács-Dajka, E., Dynamics of the fast solar tachocline II. *Astron. Astrophys.* 2003, **413**, 1143–1151.

Forgács-Dajka, E. and Petrovay, K., Tachocline confinement by an oscillatory magnetic field. *Solar Phys.* 2001, **203**, 195–210.

Forgács-Dajka, E. and Petrovay, K., Dynamics of the fast solar tachocline I. Dipolar field. *Astron. Astrophys.* 2002, **389**, 629–640.

Garaud, P., Dynamics of the solar tachocline I: An incompressible study. *Mon. Not. Roy. Astr. Soc.* 2001, **329**, 1–18.

Markiel, J.A. and Thomas, J.H., Solar interface dynamo models with a realistic rotation profile. *Astrophys. J.* 1999, **523**, 827–837.

Parker, E.N., The generation of magnetic fields in astrophysical bodies X: Magnetic buoyancy and the solar dynamo. *Astrophys. J.* 1975, **198**, 205–209.

Parker, E.N., A solar dynamo surface wave at the interface between convection and nonuniform rotation. *Astrophys. J.* 1993, **408**, 707–719.

Petrovay, K., Topological pumping in the lower overshoot layer; in *The Sun and Cool Stars: Activity, Magnetism, Dynamos*, edited by I. Tuominen, D. Moss and G. Rüdiger 1991, pp. 67–70.

Petrovay, K., What makes the Sun tick?; in *The Solar Cycle and Terrestrial Climate* 2000, pp. 3–14.

Petrovay, K., A consistent one-dimensional model for the turbulent tachocline. *Solar Phys.* 2003, **215**, 17–30.

Petrovay, K., On the possibility of a bimodal solar dynamo. *Astron. Nachr.* 2007, **328**, 777–780.

Petrovay, K. and Kerekes, A., The effect of a meridional flow on Parker's interface dynamo. *Mon. Not. Roy. Astr. Soc.* 2004, **351**, L59–L62.

Schüssler, M., On the structure of magnetic fields in the solar convective zone; in *The Hydromagnetics of the Sun*, edited by T.D. Guyenne and J.J. Hunt 1984, pp. 67–76.

Solanki, S., Inhester, B. and Schüssler, M., The solar magnetic field. *Rep. Prog. Phys.* 2006, **69**, 563–668.

Tobias, S.M., Diffusivity quenching as a mechanism for Parker's surface dynamo. *Astrophys. J.* 1996, **467**, 870–880.

Zeldovich, Y.B., Ruzmaikin, A.A. and Sokoloff, D.D., *Magnetic Fields in Astrophysics*, 1984 (New York: Gordon & Breach).

Zhang, K., Liao, X. and Schubert, G., A sandwich interface dynamo: Linear dynamo waves in the Sun. *Astrophys. J.* 2004, **602**, 468–480.